Assessment of temporal resolution of multi-detector row computed tomography in helical acquisition mode using the impulse method

メタデータ	言語: eng
	出版者:
	公開日: 2017-10-03
	キーワード (Ja):
	キーワード (En):
	作成者:
	メールアドレス:
	所属:
URL	http://hdl.handle.net/2297/43457

Title: Assessment of temporal resolution of multi-detector row computed tomography in helical acquisition mode using the impulse method

AUTHORS

Katsuhiro Ichikawa (corresponding author)

Institute of Medical, Pharmaceutical and Health Sciences, Kanazawa University 5-11-80

Kodatsuno, Kanazawa, Ishikawa 920-0942, Japan

E-mail: ichikawa@mhs.mp.kanazawa-u.ac.jp

Tel: +81-76-265-2528

Fax: +81-76-234-4366

Takanori Hara

Department of Medical Technology, Nakatsugawa Municipal General Hospital

1522-1 Komanba, Nakatsugawa, Gifu 508-0011, Japan

Atsushi Urikura

Department of Diagnostic Radiology, Shizuoka Cancer Centre

1007 Shimonagakubo, Nagaizumi, Sunto, Shizuoka 411-8777, Japan

Tadanori Takata

Department of Diagnostic Radiology, Kanazawa University Hospital

13-1 Takara-machi, Kanazawa, Ishikawa 920-8641, Japan

Kazuya Ohashi

Department of Radiology, Nagoya City University Hospital

1 Kawasumi, Mizuho-cho, Mizuho-ku, Nagoya, Aichi 467-0001, Japan

ABSTRACT

The purpose of this study was to propose a method for assessing the temporal resolution (TR) of multi-detector row computed tomography (CT) (MDCT) in the helical acquisition mode using temporal impulse signals generated by a metal ball passing through the acquisition plane. An 11-mm diameter metal ball was shot along the central axis at approximately 5 m/s during a helical acquisition, and the temporal sensitivity profile (TSP) was measured from the streak image intensities in the reconstructed helical CT images. To assess the validity, we compared the measured and theoretical TSPs for the 4-channel modes of two MDCT systems. A 64-channel MDCT system was used to compare TSPs and image quality of a motion phantom for the pitch factors P of 0.6, 0.8, 1.0 and 1.2 with a rotation time R of 0.5 s, and for two R/P combinations of 0.5/1.2 and 0.33/0.8. Moreover, the temporal transfer functions (TFs) were calculated from the obtained TSPs. The measured and theoretical TSPs showed perfect agreement. The TSP narrowed with an increase in the pitch factor. The image sharpness of the 0.33/0.8 combination was inferior to that of the 0.5/1.2 combination, despite their almost identical full width at tenth maximum values. The temporal TFs quantitatively confirmed these differences. The TSP results demonstrated that the TR in the helical acquisition mode significantly depended on the pitch factor as well as the rotation time, and the pitch factor and reconstruction algorithm affected the TSP shape.

Keywords: computed tomography, impulse signal, temporal resolution, temporal sensitivity profile

Introduction

Advances in multi-detector row computed tomography (CT) (MDCT) have resulted in continuous improvements in the temporal resolution (TR) of CT images. In particular, TR is of great interest in cardiac CT. Therefore, many investigators have examined the relations between TR and the image quality of coronary CT images among different generations of MDCT systems **[1–5]**. There are many studies related to the TR of images generated in the electrocardiogram (ECG)-gated acquisition mode for suppressing cardiac motion artefacts in lung CT images **[6–9].** However, the TRs of images obtained in the normal helical acquisition mode, which is routinely used for clinical CT examinations, have not been studied.

In CT examinations using the helical acquisition modes, body movement or breathing during the CT scanning process is sometimes unavoidable, especially in emergencies and infant cases. For such patients, a higher TR is effective in reducing motion artefacts, and it is well known that an increase in rotation speed is an effective means of improving TR. In addition, the pitch factor and the reconstruction algorithm affect TR in the helical acquisition mode because the order and arrangement of the projection data in the multi-detector helical interpolation process noticeably vary with respect to the pitch factor, and the reconstruction algorithm processes these projection data using algorithm-dependent weighting factors for helical interpolation **[10–13]**. However, since no practical methods have been proposed to measure TR for the helical acquisition mode, the effects of these parameters on it have not been investigated.

Theoretically, TR could be evaluated by examining the temporal sensitivity profile (TSP), similar to how the longitudinal (z-directional) spatial resolution can be evaluated using the section sensitivity profile (SSP), which is defined as the impulse response of

the CT system along the z-axis [13]. **Fig. 1** shows examples of theoretical TSP for a step-and-shoot CT image with full (360°) reconstruction and a single-slice helical CT image with 180° linear interpolation (180LI) [14]. In the step-and-shoot CT image, the projection data through a 360° rotation are used with a constant weighting, and thereby its TSP forms a rectangular shape as shown in **Fig. 1a**. In the single-slice helical CT with 180LI, the TSP forms a triangular shape with a base width equal to the rotation time (**Fig. 1b**). This corresponds to the triangle weight function for the helical interpolation with its base width equal to the table movement per rotation [13]. These theoretical TSPs can be easily estimated because the weighting functions are already known [14]. In contrast, it is nearly impossible to estimate theoretical TSPs of CT images of recent MDCT systems because the weighting factors are complicatedly processed in their reconstruction algorithms [15, 16], and consequently, a special software to correctly reproduce the reconstruction algorithms is needed for the theoretical TSP estimation.

To measure the SSP, a thin Al sheet or a small lead bead is usually employed, which generates an approximation of impulse signals in the z-direction [17, 18]. The SSP can then be measured from the reconstructed images with a fine table increment (typically, one-tenth of the nominal slice thickness), which are responses to the approximated impulse signal. According to this principle, a high attenuation object that briefly appears during the helical acquisition is needed to generate a temporal impulse signal for the TSP measurement.

The aim of this study is to propose a practical method for measuring the TSP of MDCT in the helical acquisition mode using a temporal impulse signal generated by a metal ball passing through the acquisition plane. The measurement procedures in the proposed

method, the comparisons between theoretical and measured TSPs, and the relationship between the TSP and image quality in a motion phantom are described in this paper.

Materials and Methods

Proposed method for the TSP measurement

As shown in **Fig. 2**, a metal ball was shot along the central rotation axis during helical acquisition at a high speed of approximately 5 m/s to provide almost simultaneous temporal impulse signals to all the detector channels. If the timing difference between the first and last MDCT detector channels is not sufficiently small compared with the width of the TSP, the approximation of the temporal impulse signal becomes insufficient, consequently causing TSP measurement errors. Therefore, the speed of the metal ball was set to be sufficiently high so that the timing difference was less than one-tenth of the width of the TSP. This is similar to how the thickness of the Al sheet or the diameter of the bead for the SSP measurements were chosen to be less than one-tenth of the full width at half maximum (FWHM) of the SSP **[17]**. It was assumed that the shortest FWHM of the TSP was 0.1 s for recent MDCTs with detector full widths of 40 mm. Thus, a metal ball speed of approximately 5 m/s, which we used in this study, should be sufficiently high because of the corresponding timing difference of 0.008 s. In most CT systems, it is possible to conduct acquisitions with the patient tables positioned away from the CT gantries. Thus, there was no collision between the patient table and launching platform from which the metal ball was shot.

The passage of the metal ball caused streaks in the reconstructed images, as shown in **Fig. 3**. Assuming that the table position at time t_0, when the metal ball passed through the acquisition plane, was defined as z_0, the image reconstructed at z_0 showed the

maximum intensity of the streak image. As the table speed during the helical acquisition was constant, the difference in z-position between each image and the image at z_0 was proportional to the time difference between them. Therefore, each image had its own time stamp, and consequently, the intensity of its streak image reflected the temporal response to the momentary attenuation caused by the passage of the metal ball through the acquisition plane. Thus, the TSP could be obtained by measuring the mean values of the regions of interest (ROIs) on the streak images within a specified z-position range. The table position (z) could be converted to time (t) to determine the TSP (t) using the following formula:

$$t = \frac{(z - z_0)R}{WP},\qquad\qquad (1)$$

where R is the rotation time (per 360° rotation), W is the detector full width and P is the pitch factor. The image reconstruction increment should be set small enough (e.g. 0.1 mm) so that the corresponding time increment of the TSP data is short enough to correctly detect the TSP shape. To obtain the normalized response values of the TSP, the background level was subtracted from the ROI values, and then, the resultant values were divided by the maximum ROI value.

Metal ball

We used a metal ball from the popular Japanese gambling machine, Pachinko. The ball was made of steel with the following regulated specifications: 11.0 mm in diameter and 5.4–5.7 g in weight. This product provided high attenuation, a fixed quality level and was large enough for the ROI measurements. An original spring-based mechanism with an adjustable speed setting was developed to shoot the metal ball from a launching

platform. After being shot, the guide rail (indicated in **Fig. 2**) guided the metal ball along the correct trajectory; i.e. aligned with the central axis of rotation of the CT system's gantry. The speed of the metal ball as it passed through the acquisition plane was determined from its average position changes per millisecond observed in high-speed movies with 1000 frames/s, recorded with a high-speed digital camera EX-FC150 (CASIO Computer Company, Tokyo, Japan). The accuracy of the metal ball speed measurement for 10 observations at the 5.0 m/s setting was 5.04 ± 0.11 m/s. Since the free-fall of the metal ball as it passed through the acquisition plane was estimated to be less than 0.4 mm for the 40 mm full width of the detectors, the position change in the vertical (y) direction caused by the free-fall was negligible.

Comparison of measured and theoretical TSPs

We used a 4-channel MDCT system, Somatom Volume Zoom (Somatom VZ; Siemens Medical Solutions, Forchheim, Germany) and a 16-channel MDCT system, Aquilion 16 (Toshiba Medical Systems, Tokyo, Japan). The reconstruction algorithm of the Somatom VZ system and helical filter interpolation (HFI) for the 4-channel mode of the Aquilion 16 system have been previously described **[11, 12],** and the weight functions for helical interpolation of these reconstruction algorithms were known. Thus, these two CT systems could be used to compare the measured and theoretical TSPs. The actual TSP measurements were conducted using our proposed method. The acquisition parameters for the Somatom VZ system were 120 kVp, 100 mA, $R = 0.75$ s, and 1 mm $\times$ 4 detector configuration, with $P = 0.675$, 1.0 and 1.5. The acquisition parameters for the Aquilion 16 system were 120 kVp, 100 mA, $R = 1.0$ s, and 2 mm $\times$ 4 detector configuration, with $P = 0.625$, 1.0 and 1.5. CT images were reconstructed with a

100-mm display field of view, and 1 mm (Somatom VZ) and 2 mm (Aquilion 16) nominal slice thicknesses. The metal ball was shot at a speed of approximately 5 m/s. We estimated the FWHM and full width at tenth maximum (FWTM) from the TSP results. The helical interpolation method for the Somatom VZ system with $P = 1.5$ and the Aquilion 16 system was 180LI, and that of the Somatom VZ system with $P = 0.675$ and 1.0 was 360° linear interpolation (360LI). The theoretical TSP was calculated using the following steps:

1. The time data relative to the central time ($t = 0$) were allocated, ranging from $-R$ to $+R$ at 0.01 s intervals;

2. The relative z-positions of four detector channels at each relative time were calculated using W, P and R;

3. The weight values of the helical interpolation for direct and complementary projections (only direct projections for 360LI) were calculated at each relative z-position, referring to the weight functions for the helical interpolation;

4. The weight values consequently allocated to each relative time were totalled;

5. The total values for all the relative times were finally normalised by their maximum value to obtain TSP.

The weight function for the Somatom VZ system was a triangle with a base width of 2.0 mm (= double the nominal slice thickness). For HFI of the Aquilion 16 system, the weight function was varied in each interpolation process as the weight values were

9

determined during the re-sampling process of the projection data and the subsequent filter interpolation process. Therefore, the weight values allocated at each relative time were calculated according to the interpolation method of HFI using a rectangular filter with a width of 2.0 mm (= the nominal slice thickness).

Effect of metal ball speed

To confirm whether a metal ball passage speed of 5 m/s would be sufficient for the recent MDCT systems, TSPs were assessed using one of the latest MDCT systems, Somatom Definition Flash (Somatom DF; Siemens Medical Solutions, Forchheim, Germany) for passage speeds of approximately 2.5, 3.5 and 5.0 m/s. Although the Somatom DF system is a dual-source MDCT system equipped with two X-ray tubes and two corresponding detectors, we employed its single-source helical mode, which is generally used for clinical examinations. The acquisition parameters were set to 120 kVp, 200 mA, 0.6 mm × 64 detector configuration, 1.0 mm nominal slice thickness, $R = 0.33$ s and $P = 0.8$. The rotation time was the shortest one in this CT system, and the pitch factor was a moderate one used clinically. The estimated impulse timing difference between the first and last channels for the passage speeds of 2.5, 3.5 and 5.0 m/s were approximately 0.015, 0.011 and 0.008 s, respectively.

TSP and image quality for a motion phantom

We investigated the effect of the TSP on the image quality of a target in motion using the Somatom DF system. An anthropomorphic foot phantom (Alderson Phantoms, Radiology Support Devices, Long Beach, CA) was moved in a horizontal (x) direction at approximately 7 mm/s during helical acquisition, as shown in **Fig. 4**. The

reproducibility of the motion speed, which was measured using the same method as the metal ball speed measurement described in the section 'Metal Ball', was 7.03 ± 0.1 mm/s for 10-times measurements. This speed was chosen so as to obtain CT images in which TR difference was well reflected as an image-blurring (motion-blurring) difference. First, the effect of the pitch factor was examined using $P = 0.6$, 0.8, 1.0 and 1.2 for $R = 0.5$ s. Then, we compared two R/P combinations of 0.33/0.8 and 0.5/1.2, which offered similar acquisition speeds of 93.09 and 92.16 mm/s, respectively. The other acquisition parameters were 120 kVp, 100 effective tube current-time product (effective mAs) and 0.6 mm × 64 detector configuration. CT images were reconstructed with a 1.0 mm nominal slice thickness and 1.0 mm table increment using a mild edge-enhancing kernel (B50f). The same effective mAs was used to equalise the image noise levels of all acquisitions. We set the metal ball speed to approximately 5.0 m/s for the TSP measurements. To validate the results of the comparison, the temporal transfer functions (TFs) were calculated from TSPs using a Fourier transformation, using the method for calculating longitudinal spatial TF from the SSP [18]. Before the Fourier transformation was applied, the TSP data were extended into 1024-point data using a zero padding technique, which provided band-limited interpolation in the frequency domain.

Results

Comparison of measured and theoretical TSPs

Figures 5 show the measured and theoretical TSPs of the Somatom VZ and Aquilion 16 systems, respectively. The measured TSPs accurately conformed to the theoretical TSPs for both systems. The FWHM/FWTM values of the Somatom VZ system for $P = 0.675$,

1.0 and 1.5 were NA/1.312 s, 0.747 s/0.899 s and 0.381 s/0.593 s, respectively (NA: not applicable). The FWHM for $P = 0.675$ could not be measured because of the flat (shoulder-like) regions in TSP at approximately half maximum level, as shown in **Fig. 5a**. The FWHM/FWTM values of the HFI of the Aquilion 16 system for $P = 0.625$, 1.0 and 1.5 were 1.531 s/1.710 s, 1.001 s/1.284 s and 0.501 s/0.791 s, respectively. The maximum differences between the measured and theoretical TSPs for FWHM and FWTM were 0.004 ($P = 0.625$, Aquilion 16 system) and 0.008 s ($P = 1.0$, Aquilion 16 system), respectively.

Effects of metal ball speed

The three metal ball speeds (2.5, 3.5 and 5.0 m/s) examined in this investigation presented almost identical widths and shapes of TSP. The FWHM/FWTM values for 2.5, 3.5 and 5.0 m/s were 0.365 s/0.429 s, 0.365 s/0.427 s and 0.364 s/0.429 s, respectively. These metal ball speeds were sufficiently high and did not affect the TSP measurement accuracy for $R = 0.33$ s with $P = 0.8$ of the Somatom DF system.

Effect of TSP on image quality for a motion phantom

Figs. 6a and b show the measured TSPs of $P = 0.6$, 0.8, 1.0 and 1.2, with $R = 0.5$ s, obtained using the Somatom DF system and the corresponding temporal TFs, respectively. Similar to the Somatom VZ and Aquilion 16 systems, the pitch factor affected the TSP width and shape. The FWHM/FWTM values of $P = 0.6$, 0.8, 1.0 and 1.2 were 0.743 s/0.835 s, 0.549 s/0.645 s, 0.434 s/0.516 s and NA/0.426 s, respectively. Both FWHM and FWTM narrowed as P increased, while the FWHM for $P = 1.2$ could not be measured because of the flat regions in the TSP at the half maximum level, which

was similar to the TSP for $P = 0.675$ from the Somatom VZ system. The 10% temporal TFs of $P = 0.6$, 0.8, 1.0 and 1.2 were 1.19, 1.61, 2.03 and 2.82 cycles/s, respectively; these results indicated that TR clearly increased with P. The temporal TFs of $P = 0.6$, 0.8, 1.0 and 1.2 decreased towards zero at 1.32, 1.80, 2.29 and 3.40 cycles/s, respectively, and then increased again. Since such increases after the drop to zero, which are called 'spurious resolutions', were not true TRs, the 10% temporal TF values were determined in frequency ranges below the respective zero-drop frequencies. **Fig. 7** demonstrates the CT image samples of the motion foot phantom for the four pitch factors. The longitudinal (slice) level of these images was located at the talocalcaneal joint in the foot phantom. This slice level was chosen because the level provided representative images that reasonably reflected the image sharpness features for the respective pitch factors. The image (motion) blurring improved with P, and the image from $P = 1.2$ had the best image quality with the least motion artefacts. Conversely, other images presented insufficient image qualities with image blurring and motion artefacts, including double or triple contours.

Figs. 8a and b show the measured TSPs of the R/P combinations of 0.33/0.8 and 0.5/1.2, which offered similar acquisition speeds, and corresponding temporal TFs, respectively. Although the FWTM values of 0.33/0.8 and 0.5/1.2 were almost identical (0.424 for 0.33/0.8 and 0.426 for 0.5/1.2), the shapes of these two R/P combinations were significantly different. The 10% temporal TFs of 0.33/0.8 (2.45 cycles/s) was lower than that of 0.5/1.2 (2.82 cycles/s). **Fig. 9** presents sample CT images of the foot phantom for the two R/P combinations. In the figure, the CT images of the phantom without motion were presented to demonstrate that the difference in R did not affect the image sharpness. For a comparison with motion, the R/P combination of 0.5/1.2

provided better image sharpness compared with the R/P combination of 0.33/0.8, while some artefacts remained in the image of 0.5/1.2. This difference seemed to be effect of the TR difference observed in the temporal TF results.

Discussion

The measured TSPs of the Somatom VZ system and the 4-channel mode of the Aquilion 16 system conformed precisely to their theoretical TSPs, demonstrating the validity of our proposed method. In addition, the TSP shape of $P = 0.625$ for the Aquilion 16 system with HFI agreed with a simulated TSP result with the same pitch factor, detector configuration and nominal slice thickness that is given in a previously published paper by the inventors of HFI **[13].** Thus, the validity of this calculation method for obtaining the theoretical TSP has also been confirmed. For $P = 1.0$ and 1.5, the TSP shapes were significantly different between the Somatom VZ and Aquilion 16 systems, indicating the dependency of the TSP on the reconstruction algorithm. As the measured TSPs of $P = 0.675$ for the Somatom VZ system and $P = 0.625$ for the Aquilion 16 system precisely reproduced the respective complicated shapes of the theoretical TSPs, it was indicated that the proposed method had sufficient temporal response. We simultaneously learned that the 5 m/s metal ball speed was sufficient for these TSP analyses using the Somatom VZ and Aquilion 16 systems.

For one of the most recent CT systems, Somatom DF, the metal ball speed of 5 m/s was sufficiently quick to generate the required results for the shortest rotation time of 0.33 s and a moderate pitch factor of 0.8. Furthermore, even when the metal ball speed was 2.5 m/s, we were able to correctly measure the TSP. This demonstrated that the timing difference (0.015 s) between the first and last detector channels satisfied the required

level of less than one tenth of the FWHM (one tenth of 0.364 s). The widest full-width detector for helical acquisition mode of the currently available systems is 80 mm of a 128-channel MDCT and a 320-channel MDCT, with a maximum rotation speed of 0.27 s and 0.275 s, respectively. For the 80-mm width, the estimated timing difference for the metal ball speed of 5 m/s is 0.016 s, which would satisfy the required levels of these MDCT systems because it appears that the narrowest FWHMs of the TSP of these MDCT systems are greater than 0.16 (0.016×10) s, except for the cardiac modes which are not covered in the purpose of our proposed method. However, a metal ball speed greater than 5 m/s may be required for systems in the near future, which will have detectors with wider full widths and higher rotation speeds.

The investigation of the effect of the TSP on the motion of the phantom image for the four pitch factors and for the two R/P combinations with the Somatom DF system revealed interesting results that demonstrated the efficacy of measuring the TSP. In the comparison among the four pitch factors ($P = 0.6$, 0.8, 1.0 and 1.2), it was easy to determine that the TSP narrowed with the increase in pitch factor. However, we faced difficulties in understanding the variation of the TSP shapes and how TR improved with the pitch factor. In contrast, the temporal TF and 10% temporal TF, calculated from the TSP, were effective in comparing the TSP in terms of the TR.

Despite the similar acquisition speeds between the R/P combinations of 0.33/0.8 and 0.5/1.2, the image sharpness of 0.5/1.2 was better than that of 0.33/0.8 for the motion target (**Fig. 9c and d**). The TSP shapes significantly differed between the two combinations, and both temporal TF and 10% temporal TF of 0.5/1.2 were better than those of 0.33/0.8, as shown in **Fig. 8.** For the comparison using width-based TR evaluation, the FWTM was almost identical between these combinations, while the

FWHM was not able to be applied due to the complicated TSP shape of 0.33/0.8. In general, the rotation time has been considered the dominant factor for determining TR performance. However, in practice, TR depends significantly on the pitch factor, and a rotation time of 0.5 s with a high pitch factor of 1.2 offered a higher TR compared with the rotation time of 0.33 s with a moderate pitch factor of 0.8. Since neither pitch factor exceeded the values used clinically, it is important for radiologists and CT operators to be aware of the pitch factor dependency of TR in terms of image quality for motion targets. Unlike the SSP for longitudinal resolution evaluation, which generally indicates only simple shapes like Gaussian or rectangular, the TSP often indicates a complicated shape as shown in our results. Thus, the temporal TF would be effective for the evaluation of the TR of CT images.

In this study, the relation among the TSP, temporal TF and CT image sharpness of the motion target was investigated for four pitch factors and two combinations of rotation time and pitch factor using one of the recent MDCT systems with 64 detector rows. Our results showed that TR performance could reasonably be evaluated using the TSP measured with the proposed method and the temporal TF calculated from it. However, TR investigations with more varieties of acquisition parameters and different CT systems are necessary to correctly confirm the efficacy of TR evaluation using the TSP. In addition, the motion speed of the phantom we examined was only approximately 7 m/s, and the motion trajectory was only linear. In a preliminary investigation, when using a phantom speed of approximately 15 m/s, the motion artefacts were too severe to compare the TRs in terms of the image appearances. However, the motion speed and trajectory did not necessarily simulate a clinical situation. Therefore, further investigations using other motion phantoms are necessary to more accurately analyse

TR performance of the helical CT images.

Conclusion

The TSP as a TR index of CT images obtained with the helical acquisition mode was able to be correctly measured using the proposed method, which involved the passage of a metal ball through the acquisition plane at a speed of approximately 5 m/s. The TSP measurements confirmed that the TR of CT images acquired using helical acquisition mode significantly depended on the pitch factor as well as the rotation time. Furthermore, the pitch factor and reconstruction algorithm affected the TSP shape. The temporal TF and 10% temporal TF, calculated from the TSP, could be effective measures for comparison of TRs especially for TSPs with different shapes.

References

[1] Ohnesorge B, Flohr T, Becker C, Kopp AF, Schoepf UJ, Baum U, et al. Cardiac imaging by means of electrocardiographically gated multisection spiral CT: initial experience. Radiology 2000;217(2):564–71.

[2] Halliburton SS, Stillman AE, Flohr T, Ohnesorge B, Obuchowski N, Lieber M, et al. Do segmented reconstruction algorithms for cardiac multi-slice computed tomography improve image quality? Herz 2003;28(1):20–31.

[3] Flohr TG, McCollough CH, Bruder H, Petersilka M, Gruber K, Süss C, et al. First performance evaluation of a dual-source CT (DSCT) system. Eur Radiol

2006;16(2):256–68.

[4] Ertel D, Kröber E, Kyriakou Y, Langner O, Kalender WA. Modulation transfer function-based assessment of temporal resolution: validation for single- and dual-source CT. Radiology 2008;248(3):1013–7.

[5] Baumüller S, Leschka S, Desbiolles L, Stolzmann P, Scheffel H, Seifert B, et al. Dual-source versus 64-section CT coronary angiography at lower heart rates: comparison of accuracy and radiation dose. Radiology 2009;253(1):56–64.

[6] Schoepf UJ, Becker CR, Bruening RD, Helmberger T, Staebler A, Leimeister P, et al. Electrocardiographically gated thin-section CT of the lung. Radiology 1999;212(3):649–54.

[7] Montaudon M, Berger P, Blachère H, De Boucaud L, Latrabe V, Laurent F. Thin-section CT of the lung: influence of 0.5-s gantry rotation and ECG triggering on image quality. Eur Radiol 2001;11(9):1681–7.

[8] Boehm T, Willmann JK, Hilfiker PR, Weishaupt D, Seifert B, Crook DW, et al. Thin-section CT of the lung: does electrocardiographic triggering influence diagnosis? Radiology 2003;229(2):483–91.

[9] Hofmann LK, Zou KH, Costello P, Schoepf UJ. Electrocardiographically gated 16-section CT of the thorax: cardiac motion suppression. Radiology

2004;233(3):927–33.

[10] Hu H. Multi-slice helical CT: scan and reconstruction. Med Phys 1999;26(1):5–18.

[11] Schaller S, Flohr T, Klingenbeck K, Krause J, Fuchs T, Kalender WA. Spiral interpolation algorithm for multislice spiral CT--part I: theory. IEEE Trans Med Imaging 2000;19(9):822–34.

[12] Taguchi K, Aradate H. Algorithm for image reconstruction in multi-slice helical CT. Med Phys 1998;25:550–561.

[13] Taguchi K, Anno H. High temporal resolution for multislice helical computed tomography. Med Phys 2000;27(5):861–72.

[14] Polacin A, Kalender WA, Marchal G. Evaluation of section sensitivity profiles and image noise in spiral CT. Radiology 1992;185(1):29–35.

[15] Hein I, Taguchi K, Silver MD, Kazama M, Mori I. Feldkamp-based cone-beam reconstruction for gantry-tilted helical multislice CT. Med Phys 2003;30(12):3233–42.

[16] Flohr T, Stierstorfer K, Bruder H, Simon J, Polacin A, Schaller S. Image reconstruction and image quality evaluation for a 16-slice CT scanner. Med Phys 2003;30(5):832–45.

[17] Hsieh J. Slice-Sensitivity Profile and Noise, In: Computed Tomography—Principles, Design, Artifacts and Recent Advances, Washington Bellingham: SPIE; 2003, p. 348–54.

[18] Wang G, Vannier MW. Longitudinal resolution in volumetric X-ray computerized tomography--analytical comparison between conventional and helical computerized tomography. Med Phys 1994;21(3):429–33.

Figure captions

Figure 1

TSPs of (a) a step-and-shoot acquisition image and (b) a single helical acquisition image with 180LI.

The base widths of both TSPs are equal to the rotation time R.

Figure 2

Schematic of the proposed TR measurement method and a photo of the launching platform. A metal ball was shot along the central axis of rotation at a high speed during helical acquisition. The metal ball almost simultaneously provided temporal impulse signals to all the detector channels.

Figure 3

Streak images caused by a passage of metal ball and their corresponding points on TSP.

The intensities of the streaks corresponded to the temporal sensitivities to the impulse signal. The table position of each image was converted to each time point in the TSP using the scale conversion formula (1).

Figure 4

Anthropomorphic foot phantom placed on a hand made plastic board equipped with a mechanism for the phantom motion. The plastic board was on the patient table of the CT system. During helical acquisition, the foot phantom was moved in the z-direction, due to the table feed for the helical acquisition, and simultaneously moved in the horizontal (x) direction (black arrow), by the force from the phantom motion mechanism.

Figure 5

Measured and corresponding theoretical TSPs for (a, b, c) the Somatom VZ system with a 1 mm × 4 detector configuration and a nominal slice thickness of 1 mm, and (d, e, f) the 4-channel mode of Aquilion 16 system with a 2 mm × 4 detector configuration and a nominal slice thickness of 2 mm.

Figure 6

(a) Measured TSPs for pitch factors of 0.6, 0.8, 1.0 and 1.2 with a rotation time of 0.5 s and (b) the corresponding temporal TFs.

Figure 7

Sample CT images of an anthropomorphic foot phantom that was moved at
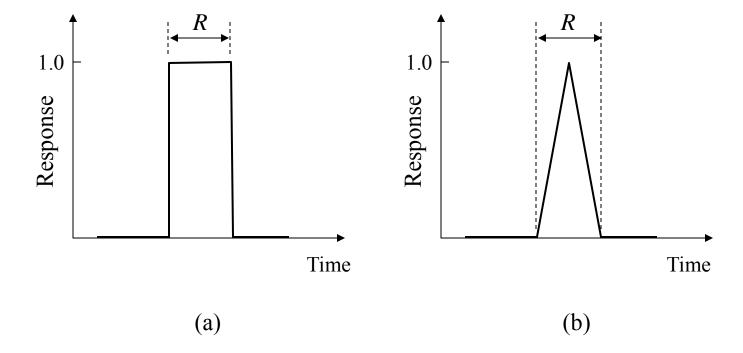
approximately 7 mm/s in the horizontal direction during helical acquisition with pitch factors of (a) 0.6, (b) 0.8, (c) 1.0 and (d) 1.2 in the Somatom DF system.
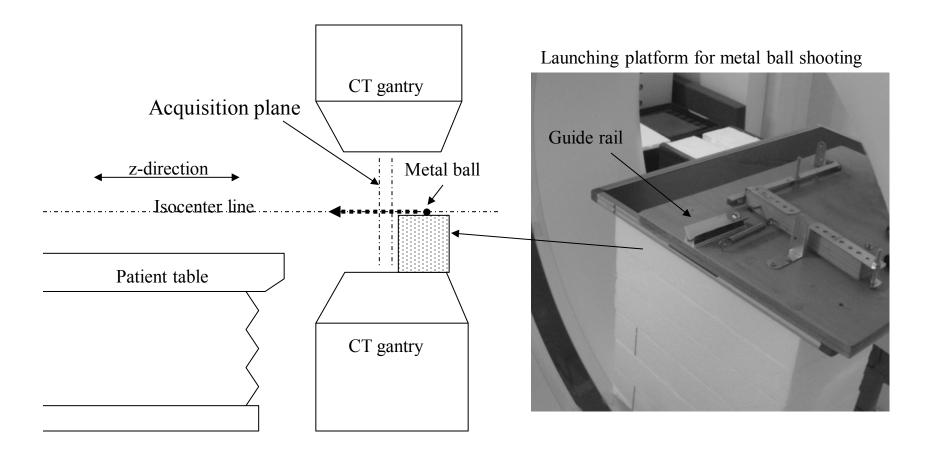
Figure 8

(a) Measured TSPs for the R/P combinations of 0.5/1.2 and 0.33/0.8 in the Somatom DF system and (b) the corresponding temporal TFs.

Figure 9

Sample CT images of an anthropomorphic foot phantom for R/P combinations of (a, c) 0.33/0.8 and (b, d) 0.5/1.2, without and with motion. The upper two images of the phantom without motion for (a) 0.33/0.8 and (b) 0.5/1.2 are displayed to demonstrate that the difference in rotation time did not affect the image sharpness.
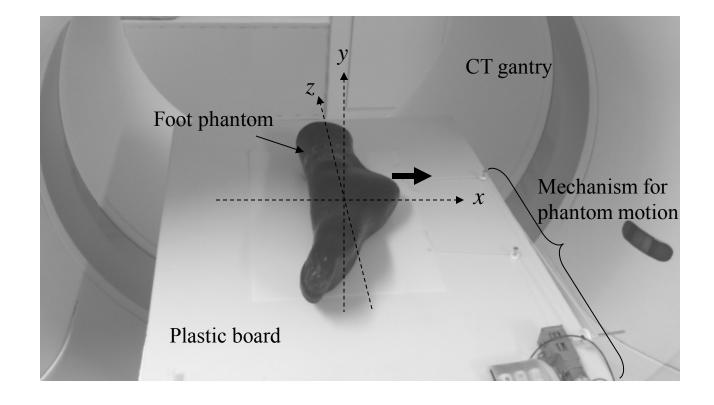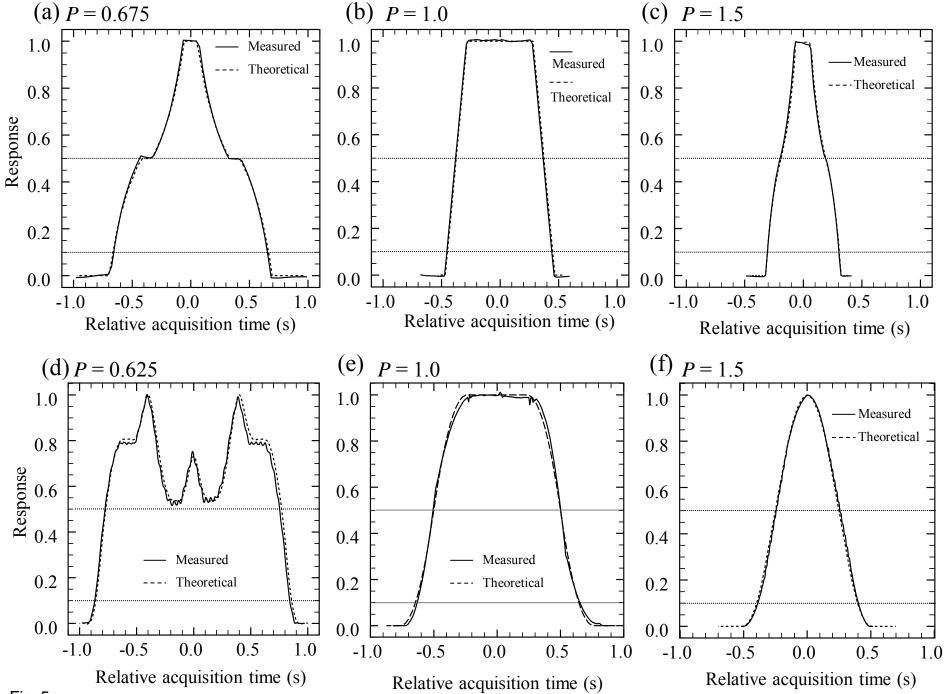
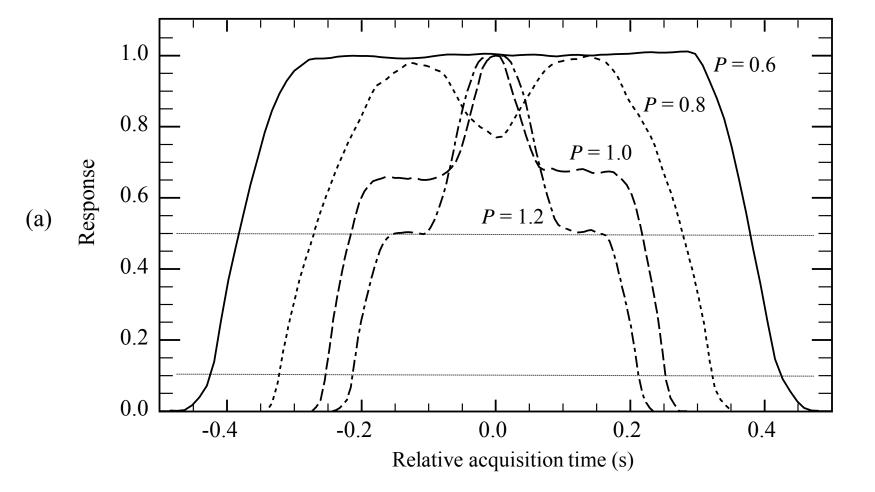(a)   (b)

Fig. 1

Launching platform for metal ball shooting

CT gantry

Acquisition plane

z-direction

Isocenter line

Metal ball

Patient table

CT gantry

Guide rail

Fig. 2

ROI

TSP

Relative time

0

z_0

z-position

Fig. 3

Fig. 4

(a) $P = 0.675$

(b) $P = 1.0$

(c) $P = 1.5$

(d) $P = 0.625$

(e) $P = 1.0$

(f) $P = 1.5$

Fig. 5

(a)

Response

Relative acquisition time (s)

$P = 0.6$

$P = 0.8$

$P = 1.0$

$P = 1.2$

Fig. 6 (a)

(b)

Temporal TF

Frequency (cycles/s)

$P = 1.0$

$P = 1.2$

$P = 0.8$

$P = 0.6$

Fig. 6(b)

(a)

(b)

(c)

(d)

Fig. 7

(a)

Fig. 8(a)

(b)

Temporal TF

0.5/1.2

0.33/0.8

Frequency (cycles/s)

Fig. 8(b)

Fig. 9